Calculation of solar radiation arriving to the outer fringe based on astronomical ephemerides DE 406.

V. M. Fedorov, A.A. Kostin

Introduction

Solar radiation arriving to the Earth alters both in time and space. Variation of arriving solar radiation is determined by two basic reasons, which have different physical nature. First, solar radiation variations are determined by the Sun physical activity shift (Willson, 1982; Frohlich, 1989; Frohlich et al., 1998; Makarova et al., 1991; Foukal et al., 2006; Willson, Mordvinov, 2003; http://www.sidc.be/; http://www.pmodwrc.ch/). The said variations are not considered in our calculations. Second, variations of solar radiation arriving to the Earth are determined celestially, by mechanical processes. These variations of solar stream, until the present day, have been basically studied in geological scale of time which is known to be rather sustained. Calculations of solar radiation, however, do not cover such astronomical elements, exposed to secular perturbations, as longitude of perihelion, ellipticity, Earth's axis inclination, which have long (tens of thousands years) periods of variations. Periodical perturbations of the Earth's orbit elements in this case are not considered (Milankovich, 1939; Brouwer, Van Woerkom, 1950; Sharaf, Budnikova, 1969; Vulis, Monin, 1979; Berger, Loutre, 1991, Monin, Shishkov, 2000). Calculations within the range of the Earth's orbit elements periodical perturbations and solar radiation variations connected with them, were started in A. I. Voyeikov Main Geophysical Observatory (Borisenkov, 1983). However, this research did not result in any further development. Though, calculations of solar radiation arriving to the outer fringe are believed to be of importance, since the acquired values are an initial basis for the Earth radiation balance and its specific geospheres.

Opposed to the approach of M. Milankovich (Milankovich, 1939) and his successors (Brouwer, Van Woerkom, 1950; Sharaf, Budnikova, 1969; Vulis, Monin, 1979; Berger, Loutre, 1991), who considered long-term intervals of time, we made a point of a more detailed calculation for solar radiation arriving over a shorter time interval. In which case, we took into account the Earth's orbit elements and Earth axis inclinations periodical perturbations.

Basic ideas of our approach are: distance from the Earth to the Sun and Earth axis orientation are taken from NASA's accurate model DE-406 (http://ssd.jpl.nasa.gov), Earth ellipsoid is divided into latitudinal bands, and each tropical year—into segments, and each pair (band, segment) is associated with an integral (J) of insolation (W/m^2) to a band from end to end of a segment. By dividing the integral by a band square we obtain specific energy (J/m^2), collected by a band within a segment. By multiplying the integral by ratio of a band fragment length to the band length we obtain assessed value of energy (J), collected by this fragment within the segment.

To calculate the said values, a number of theoretical simplications was introduced. Basic simplications: solar activity is considered constant, irradiation—coming from the centre of the Sun, Earth atmosphere influence is ignored. All theoretical simplications are stated in section 1. Pure formulae for calculations are given in section 2. Tried technology of rough calculations and their typical tolerance are discussed in section 3. Tendencies of arriving solar radiation variation are discussed in section 4.

1. The selected approach towards description of arriving solar radiation

Considered period of time is from 3000 BC to 2999 AD. The Earth's surface approximates ellipsoid, hereinafter referred to as MRS80, swaying against geoid, with major semiaxes lengths of $p_1=p_2=A$=6378137 m and minor semiaxis length of $p_3=B$=6356752 m. Minor semiaxis at each moment lies in the Earth's axis, and ellipsoid centre—in geocenter. Semiaxes lengths with rounding to one meter correspond to parameters of overall Earth ellipsoid GRS80, which is fixed relative to geoid[1].

(1) parameters of GRS80 (Geodetic Reference System 1980) are recommended for use by International Union of Geodesy and Geophysics in 1980. Definition of MRS80: Moving Reference System 1980.

Swaying ellipsoid MRS80 is provided with imaginary scale of parallels and meridians, system of normals and geodetic coordinates, whereby vertical lines, horizontal planes and latitudinal zones of Earth are determined. These lines, planes and zones together with ellipsoid slightly sway against the geoid.

Swayings are connected with the Earth's axis inclination from its midposition within the Earth body. Inclinations have been registered from the end of the 19th century in terms of geographic poles movement[2].

(2) Each of geographic poles moves against the geoid along a multiturn open curve which fits within a 30m square. One turn (Chendler's cycle) lasts for about 14 months.

Swaying ellipsoid has been chosen instead of a fixed one for two reasons: first: to avoid adding complexity to calculations, and because of the lack of a sound swaying model, which would embrace the whole time span examined.

In the absence of obstacles for rays, solar radiation which achieves a given point of the Earth surface, in general, will be resolved on vertical (normally against the surface) and horizontal (horizontal tangent against the surface) constituents. Vertical constituent hereinafter will be referred to as falling vertical radiation (FVR).

We consider a model of solar radiation and its imaginary measurement on the Earth's surface according to which:

1) isotropic radiation comes to the Earth from the center of the Sun[3],

---

(3) Hence, the solar radiation power density decreases as the inverse square of the distance from the center of the Sun.

---

2) eclipses are ignored,
3) radiation power density at a distance of 1 A.U. from the center of the Sun at each moment equals to u_0=1367 W/m^2, where 1 A.U. =r_0=149597870691 m,
4) dissipating effect of the atmosphere is ignored,
5) the Earth's surface is substituted with swaying ellipsoid MRS80.

Swaying ellipsoid is split into Δ-degree longitudinal bands (geodetical latitude is implied)[4], where $\Delta \in \{1, 5\}$.

---

(4) Projection of each band against the geoid "floats" in relations to the geoid (type of movement is various ring displacements), departing from its midposition as much as 15 meters in accordance with Chendler cycles.

FVR integrals are calculated – energy (in Joules), arriving to the Earth via each of the bands in each of the L segments within each tropical year examined, where $L \in \{12, 360\}$, and linear combinations of these integrals (tropical decades, months, quarters, half-years, years).

Tropical years were chosen instead of calendar years to avoid the four-year calendar rhythmics. Number of a tropical year aligns with the number of the calendar year within which it starts. Tropical year stands for projective tropical year tracked by movement of the Sun projection against ecliptic. If L is a number of segments into which a projective tropical year shall be divided, an n^{th} segment starts at the moment when ecliptic longitude of the Sun adopts a value of $360(n–1)/L$ (in degrees).

To take account of day elongation due to gradual slow-down of the Earth rotation we differentiate the calendar time scale within which a single day corresponds to a massive of 86400 calendar seconds, and scale of uniformly running time, according to which daily intervals are measured in true seconds and are not equal to each other. Solar radiation integrals are calculated according to scale of uniformly running time.

Imaginary clock keeping account of uniformly running time is situated in the center of the Earth. An event on a small area of the Earth ("a dose of solar radiation arrived") is related to the axle of uniformly running time in the following way. We assume a moment of a corresponding dose bundle imaginary start from the center of the Sun. A dose directed towards the center of the Earth is deposited from this bundle. A moment of imaginary arrival of this dose to the Earth's center is calculated (assuming absence of obstacles on its way). This arrival moment is selected as the one to which the said event shall be related to.

Small (20-40ms) delays (various in various areas of a band) may emerge for this way of relation. Although, from the point of view of large scale Earth processes such systematic delays of relation are omissible. They are equivalent to small (about 30ms) displacements of tropical years segments boundaries. A variant with delays has been chosen for the reason that their exclusion could result in excessive complication of calculations.

2. Pure Formulae for Calculations

According to the chosen model of solar radiation and its measurement, calculation of FVR integrals (in Joules) leans upon calculation of vertical insolation $\Lambda(t,\varphi,\alpha)$ (W/m^2), which would be observed in the absence of the Earth atmosphere in a specific moment, in a specific point of MRS80. Here t is a moment at the scale of uniformly running time (c), φ and α – expressed in radians geodetic latitude (in relation to MRS80) and sliding longitude (clocking angle transferred into radians) are the points of imaginary measurement of FVR.

Elementary fragment of a tropical year may be obtained via its splitting into 360 parts. FVR energy, arriving to the Earth via a band of enclosing surface, limited by latitudes φ_1 and φ_2 (in radians), in n^{th} elementary fragment of m^{th} tropical year, let us designate as $I_{\text{nm}}(\varphi_1,\varphi_2)$. FVR energy, arriving via the same band within the q^{th} segment of m^{th} tropical year, let us designate as $J_{\text{qm}}(\varphi_1,\varphi_2)$. We have

$$L = 360 \Rightarrow J_{qm}(\varphi_1,\varphi_2) = I_{qm}(\varphi_1,\varphi_2)\,,\quad L = 12 \Rightarrow J_{qm}(\varphi_1,\varphi_2) = \sum_{n=30(q-1)+1}^{30q} I_{nm}(\varphi_1,\varphi_2) \qquad (1)$$

Let us assume that t_{nm1} and t_{nm2} is the beginning and the end of n^{th} elementary fragment of m^{th} tropical year on the scale of uniformly running time (c). In this case

$$I_{nm}(\varphi_1,\varphi_2) = \int_{t_{nm1}}^{t_{nm2}} \left(\int_{\varphi_1}^{\varphi_2} \sigma(\varphi) \left(\int_{-\pi}^{\pi} \Lambda(t,\varphi,\alpha)\, d\alpha \right) d\varphi \right) dt \qquad (2)$$

where $\sigma(\varphi)$ is an areal multiplier at the position of imaginary measurement of solar radiation. With its help we can calculate $\sigma(\varphi)d\alpha d\varphi$ – square (m^2) of an eternally small trapezium on ellipsoid MRS80. Length of trapezoid median (along local parallel): $q_1(\varphi)d\alpha$, trapezoid altitude (along local meridian): $q_2(\varphi)d\varphi$. We have

$$\sigma(\varphi)=q_1(\varphi)q_2(\varphi),\ q_1(\varphi)=\frac{A^2}{B}h(\varphi)\cos\varphi,\ q_2(\varphi)=\frac{A^2}{B}h^3(\varphi) \tag{3}$$

$$h(\varphi)=\frac{1}{\sqrt{1+\varepsilon^2\cos^2\varphi}},\ \varepsilon^2=\left(\frac{A}{B}\right)^2-1 \tag{4}$$

Let $b(t)$ be a moment of start from the center of the Sun of an imaginary light impulse achieving the Earth's center at the moment t. Let us assume that in the moment $b(t)$, $r(t)$ is the distance (m) between centres of the Sun and the Earth, $\gamma(t)$ is declination of the center of the Sun in radians, $\lambda(t)$ is ecliptic longitude of the center of the Sun in degrees. Subsequently

$$\lambda(t_{nm1})=n-1,\ \lambda(t_{nm2})=n \tag{5}$$

$$\Lambda(t,\varphi,\alpha)=u_0\left(\frac{r_0}{r(t)}\right)^2\max\left(\frac{D_0(t,\varphi)+D_1(t,\varphi)\cos\alpha}{\left(C_0(t,\varphi)-C_1(t,\varphi)\cos\alpha\right)^{3/2}},0\right) \tag{6}$$

$$D_0(t,\varphi)=\sin(\varphi)\sin\gamma(t)-\frac{B}{r(t)h(\varphi)},\ D_1(t,\varphi)=\cos(\varphi)\cos\gamma(t) \tag{7}$$

$$C_0(t,\varphi)=1-\frac{2Bh(\varphi)\sin(\varphi)\sin\gamma(t)}{r(t)}+\frac{B^2+\varepsilon^2A^2h^2(\varphi)\cos^2\varphi}{r^2(t)} \tag{8}$$

$$C_1(t,\varphi)=\frac{2A^2h(\varphi)\cos(\varphi)\cos\gamma(t)}{Br(t)} \tag{9}$$

$$A=6378137,\ B=6356752,\ r_0=149597870691,\ u_0=1367 \tag{10}$$

Before integrating by formula (2), it would be useful to ask yourself: if t, φ are specified, then at which α VFR would exist? Range of α, from the interval (−π,π), at which VFR would be observed, is determined by inequation $|\alpha|<\alpha_M(t,\varphi)$, where $\alpha_M(t,\varphi)$ is a limit of FVR observability at a specified latitude φ. If a specified latitude φ is close to 0, then α_m at measurement of t will fluctuate within small locality π/2. In case of specified latitude module increment, amplitude of oscillation α_m will increase. If $|\varphi|$ is close to π/2, then interval of oscillation α_m will spread from 0 to π, in which case α_m will take extreme values and, will dwell on them. In periods, when $\alpha_m = 0$, at the specified latitude there will be polar night. Within periods, when $\alpha_m = \pi$, at the specified latitude there will be polar day.

If $\alpha_ь = 0$, then FVR at specified values of t,φ will not be observed. In this case, vertical insolation at α=0 equals to 0. If $\alpha_m>0$, then with increase of |α| vertical insolation decreases from positive maximum at α=0 to some minimum at $|\alpha| = \alpha_m$. If $\alpha_m<\pi$, then the minimum equals to 0. If $\alpha_m = \pi$, then the minimum will either be equal to 0, or more than 0 (between the start and the end of polar day). In the second case FVR exists not only at $|\alpha|<\alpha_m$, but also at $|\alpha|=\alpha_m$.

One of the properties of vertical insolation is evenness by α: $\Lambda(t,\varphi,\alpha) = \Lambda(t,\varphi,-\alpha)$. Taking this property into account, formula (2) may be modified to a form which is more convenient for calculation

$$I_{nm}(\varphi_1,\varphi_2)=\int_{t_{nm1}}^{t_{nm2}} u_0\left(\frac{r_0}{r(t)}\right)^2\left(\int_{\varphi_1}^{\varphi_2}\frac{2\sigma(\varphi)}{C^{3/2}_0(t,\varphi)}\left(\int_0^{\alpha_M(t,\varphi)}\frac{D_0(t,\varphi)+D_1(t,\varphi)\cos\alpha}{(1-E(t,\varphi)\cos\alpha)^{3/2}}d\alpha\right)d\varphi\right)dt \quad (11)$$

$$\alpha_M(t,\varphi)=\arccos\left(\max\left(-1,\min\left(-\frac{D_0(t,\varphi)}{D_1(t,\varphi)},1\right)\right)\right) \quad (12)$$

$$E(t,\varphi)=C_1(t,\varphi)/C_0(t,\varphi)\,,\quad 0<E(t,\varphi)<10^{-4} \quad (13)$$

3. Approximate calculation and their errors in case of *Δ*=5, *L*=12

3.1. Plan of calculations

Calculations by formulae (1), (3)-(13) cannot be made with absolute accuracy. Inaccuracies are peculiar for initial data, procedures of interpolation and search of equation roots during processing of initial data and integration procedures.

For a variant when *Δ*=5, *L*=12 we have tried the following system of approximate calculation, corresponding to formulae (1), (3)-(13).

The first stage is a work marking of the used time scales, addressing to the HORIZONS NASA internet-service (http://ssd.jpl.nasa.gov/?horizons_doc#specific_quantities; Giorgini et al., 1996) and acquisition of primary initial data, associated with starts of days GMT. Primary data, the Earth-Sun distance (km), declination and ecliptic longitude of the Sun (degrees), and path difference (c) uniformly flowing and discontinued (adjustable) worldwide time.

The second stage is calculation of displacements of tropic years elementary fragments starts and ends in relation to starts of days GMT (for this, search of equations roots with participation of ecliptic longitude) and, at this basis, gathering of secondary initial data, associated with starts, ends and intermediate moments of elementary fragments of tropic years (for this there is interpolation of primary data). Secondary initial data are: distance Earth-Sun (m), declination of the Sun (radians), and durations of fragments (c) at the scale of uniformly flowing time.

The third stage is calculation of FVR integrals by means of secondary initial data (for this there is calculation of auxiliary variables and their substitution into integration procedures).

3.2. Three time scales and their work marking

There are three scales used: CT (Coordinate Time – coordinate, the same as uniformly flowing time), UT1 (Universal Time Without Correction – continuous worldwide time) and UT2=UTC (Universal Time With Correction – discontinuous worldwide time). Scale UT2 results from scale UT1 by episodical (once in several years) movements by ±1 calendar second for path aligning of UT2-clock with CT-clock (since 1962).

Measurement unit of scale CT is a true second. At CT scale there are two markings: tropical and calendar. Tropical marking consists of main moments $\{t_{\mathrm{nm1}}, t_{\mathrm{nm2}}\}$ – starts and ends of tropic years elementary fragments and intermediate moments $\{t_{\mathrm{nm4/3}}, t_{\mathrm{nm5/2}}\}$:

$$q\in\{4/3,5/3\} \Rightarrow t_{\mathrm{nmq}}= t_{\mathrm{nm1}} + (q-1)\,(t_{\mathrm{nm2}}-t_{\mathrm{nm1}}) \tag{14}$$

Tropic marking spreads from the first fragment of tropic year 3000BC till the last fragment of tropic year 2999AD. True duration d_{nm} (in true seconds) of n^{th} fragment m^{th} of tropic year equals to

$$d_{\mathrm{nm}} = t_{\mathrm{nm2}} - t_{\mathrm{nm1}} \tag{15}$$

Calendar marking $\{t_{\mathrm{k}}\}$ consists of starts of days GMT: zero day corresponds to data 3000BC-02-23, hereafter continuous numbering till the date 3000AD-05-05. Moments $\{t_{\mathrm{k}}\}$, specified at the scale CT, correspond to moments $\{T_{\mathrm{1k}}\}$ at scale UT1 and moments $\{T_{\mathrm{2k}}\}$ at scale UT2 (calendar seconds are counted by these scales):

$$T_{\mathrm{1k}} = 86400k,\ T_{\mathrm{2k}} - T_{\mathrm{2(k-1)}} - (T_{\mathrm{1k}}-T_{\mathrm{1(k-1)}})\in\{-1,0,1\} \tag{16}$$

Further we use functions $\tau_1(\cdot)$ and $\tau_2(\cdot)$:

$$i \in \{1,2\} \Rightarrow \tau_i(t_k) = t_k - T_{ik} - (t_{k-1} - T_{i(k-1)}) + 86400 \tag{17}$$

Their sense: $\tau_1(t_{\mathrm{k}})$ – accurate, $\tau_2(t_{\mathrm{k}})$ – approximate duration of a day with number k in true seconds,

$$\tau_2(t_{\mathrm{k}})-\tau_1(t_{\mathrm{k}})\in\{-1,0,1\} \tag{18}$$

Sequence $\{t_{\mathrm{k}}-T_{\mathrm{2k}}\}$ is a part of primary initial data. For acquisition of $\{\tau_1(t_{\mathrm{k}})\}$ at each k we calculate $\tau_2(t_{\mathrm{k-2}})$, $\tau_2(t_{\mathrm{k-1}})$, $\tau_2(t_{\mathrm{k}})$, $x_{\mathrm{k}}=|\tau_2(t_{\mathrm{k-1}})-\tau_2(t_{\mathrm{k}})|$ and perform an assignment:

$$\tau_1(t_k) = \begin{cases} \tau_2(t_k), & (x_k < 0.5) \vee (x_{k-1} \ge 0.5) \\ \tau_2(t_{k-2}) + 2(\tau_2(t_{k-1}) - \tau_2(t_{k-2})), & (x_k \ge 0.5)\,\&\,(x_{k-1} < 0.5) \end{cases} \tag{19}$$

3.3. Retrieval of primary initial data

Primary initial data is a block of values of type $r(t_{\mathrm{k}})/1000$, $(180/\pi)\gamma(t_{\mathrm{k}})$, $(180/\pi)\lambda(t_{\mathrm{k}})$, $t_{\mathrm{k}}-T_{\mathrm{2k}}$. Here $r/1000$ is a distance between centers of the Sun and the Earth in kilometers, $180\gamma/\pi$ and $180\lambda/\pi$ declination and ecliptic longitude of the center of the Sun in degrees, $t_{\mathrm{k}}-T_{\mathrm{2k}}$ – path difference of CT-clock and UT2-clock in seconds. As it was mentioned in section 2, values $r(t)$, $\gamma(t)$, $\lambda(t)$, registered at the moment t, refer to an earlier moment $b(t)$ (adjustment for running of a light impulse from the center of the Sun to the center of the Earth).

Primary initial data was retrieved by us from ephemerides NASA DE406 by means of the HORIZONS internet-service. In the inquiries made we set the following parameters (for *Time Span* there is an example):

Ephemeris Type = OBSERVER,
Target Body = Sun [Sol] [10],
Observer Location = Geocentric [500],
Time Span = Start=2001-01-01, Stop=2200-12-31, Step=1 d
*Table Settings = QUANTITIES=2,20,30,31; extra precision=YES***.**

3.4. Calculation of secondary initial data by primary data

Secondary initial data is a block of values of the type $r(t_{nmq})$, $\gamma(t_{nmq})$, d_{nm}, where $q\in\{1,4/3,5/3,2\}$. Secondary data is calculated by primary data by means of plain spline interpolation (continuous is both the spline itself, and its first and second derivative). Formulae of spline-interpolation:

$$f_M = f(x_M), f_0 = f(x_0), f_1 = f(x_1), f_2 = f(x_2),\ x_0 \le x \le x_1,\ u = (x-x_0)/(x_1-x_0) \qquad (20)$$

$$(0 < x_0 - x_M = x_1 - x_0 = x_2 - x_1,\ x_0 \le x \le x_1) \Rightarrow f(x) \approx \mathrm{spl}(f_M, f_0, f_1, f_2, u) \qquad (21)$$

$$spl(f_M, f_0, f_1, f_2, u) = d_0 + d_1 u + d_2 u^2 + d_3 pol(u) \qquad (22)$$

$$d_0 = f_0,\ d_1 = \frac{f_1 - f_M}{2},\ d_2 = \frac{f_1 - 2f_0 + f_M}{2},\ d_3 = \frac{f_2 - 3f_1 + 3f_0 - f_M}{2} \qquad (23)$$

$$pol(u) = \frac{-31u^3 + 35u^4 + 21u^5 - 35u^6 + 10u^7}{12} \qquad (24)$$

Formulae of spline-interpolation application:

$$\lambda_M(n,t) = \begin{cases} \lambda(t) - 2\pi, & (\pi \le \lambda(t))\ \&\ (n \le 3) \\ \lambda(t), & (\lambda(t) < \pi) \vee (3 < n) \end{cases} \qquad (25)$$

$$\lambda_P(n,t) = \begin{cases} \lambda(t) + 2\pi, & (\lambda(t) \le \pi)\ \&\ (358 \le n) \\ \lambda(t), & (\pi < \lambda(t)) \vee (n < 358) \end{cases} \qquad (26)$$

$$j = j(n,m,q),\ \lambda_M(n,t_j) \le \pi(n+q-2)/180 \le \lambda_P(n,t_{j+1}) \qquad (27)$$

$$r(t_{nmq}) = spl(r(t_{j-1}), r(t_j), r(t_{j+1}), r(t_{j+2}), u_{nmq}) \qquad (28)$$

$$\gamma(t_{nmq}) = spl(\gamma(t_{j-1}), \gamma(t_j), \gamma(t_{j+1}), \gamma(t_{j+2}), u_{nmq}) \qquad (29)$$

$$\tau_1(t_{nm2}) = spl(\tau_1(t_{j-1}), \tau_1(t_j), \tau_1(t_{j+1}), \tau_1(t_{j+2}), u_{nm2}) \qquad (30)$$

$$d_{nm} = ((j(n,m,2) + u_{nm2}) - (j(n,m,1) + u_{nm1}))\tau_1(t_{nm2}) \qquad (31)$$

where u_{nmq} is the equation root

$$\lambda(t_{nmq}) = \frac{\pi(n+q-2)}{180} = spl(\lambda_M(n,t_{j-1}), \lambda_M(n,t_j), \lambda_P(n,t_{j+1}), \lambda_P(n,t_{j+2}), u_{nmq}) \qquad (32)$$

Root of each equation of the type (32) is sought by approximation method with a roughness of 10^{-9} (in a day).

3.5. Calculation of FVR integrals by means of secondary initial data

After pass from (2) to (11), further siplification consists in approximate analytic integral evaluation by α. Employing decomposition

$$\frac{1}{(1-x)^{3/2}} = 1 + \frac{3}{2}x + \frac{15}{8}x^2 + \frac{35}{16}x^3 + \frac{315}{128}x^4 + Q_5(x) \tag{33}$$

$$0 < x < 10^{-4} \Rightarrow 0 < Q_5(x) < 2.71x^5 \tag{34}$$

and omitting, for short, arguments t, φ of the above introduced functions α_m , D_0, D_1, E, and auxiliary functions μ, F_0, h_0, …, h_5, we find

$$\int_0^{\alpha_M} \frac{D_0 + D_1\cos\alpha}{(1 - E\cos\alpha)^{3/2}} d\alpha = (1+\mu)F_0,\ 0 < \mu < 3\cdot 10^{-20},\ \ F_0 = h_0\alpha_M + \sum_{j=1}^{5}\frac{h_j}{j}\sin(j\alpha_M) \tag{35}$$

$$h_0 = \frac{3E}{4}\left(1 + \frac{35}{32}E^2\right)D_1 + \left(1 + \frac{15}{16}E^2 + \frac{945}{1024}E^4\right)D_0 \tag{36}$$

$$h_1 = \left(1 + \frac{45}{32}E^2 + \frac{1575}{1024}E^4\right)D_1 + \frac{3E}{2}\left(1 + \frac{35}{32}E^2\right)D_0 \tag{37}$$

$$h_2 = \frac{E}{4}\left(3 + \frac{35}{8}E^2\right)D_1 + \frac{15E^2}{16}\left(1 + \frac{21}{16}E^2\right)D_0,\quad h_3 = \frac{15E^2}{32}\left(1 + \frac{105}{64}E^2\right)D_1 + \frac{35}{64}E^3 D_0 \tag{38}$$

$$h_4 = \frac{35E^3}{128}\left(D_1 + \frac{9}{8}ED_0\right),\ h_5 = \frac{315E^4}{2048}D_1 \tag{39}$$

During integration $(1+\mu(t,\varphi))F_0(t,\varphi)$ by φ and by t the summand $\mu(t,\varphi)$ due to its smallness will be dropped out:

$$I_{nm}(\varphi_1,\varphi_2) \approx \int_{t_{nm1}}^{t_{nm2}} F_2(t)dt,\ F_2(t) = u_0\left(\frac{r_0}{r(t)}\right)^2\left(\int_{\varphi_1}^{\varphi_2} F_1(t,\varphi)d\varphi\right) \tag{40}$$

$$F_1(t,\varphi) = \frac{\sigma(\varphi)}{C_0^{3/2}(t,\varphi)}F_0(t,\varphi) \tag{41}$$

Before integration by φ, its extremes shall be specified (not to pass in vain the values of φ, whereby α_m=0). Pair (φ_1,φ_2) will be changed by the pair $(\varphi_{1m},\varphi_{2m})$ and in case of $\varphi_{1M}<\varphi_{2M}$ we shall calculate the integration pace $(\varphi_{2M}-\varphi_{1M})/set$, approximately by 1 degree. Omitting, for short, the argument t of the above introduced functions r, γ and auxiliary functions F_1, φ_{1M}, φ_{2M}, γ_H, γ_B, η, η_H, η_{H1}, η_{H2}, η_B, η_{B1}, η_{B2}, we find, that

$$\gamma_B = \arcsin\frac{B}{r},\ \gamma_H = -\gamma_B,\ \eta(x) = \arcsin\frac{B\sqrt{1+\varepsilon^2\sin^2(\gamma+x)}}{r} \tag{42}$$

$$\gamma \le \gamma_H \Rightarrow \varphi_{1M} = \varphi_1\,,\ \gamma > \gamma_H \Rightarrow \varphi_{1M} = \max\left(\varphi_1, -\frac{\pi}{2} + \gamma + \eta_H\right),\ \eta_H = \eta(\eta_H) \tag{43}$$

$$\gamma \ge \gamma_B \Rightarrow \varphi_{2M} = \varphi_2\,,\ \gamma < \gamma_B \Rightarrow \varphi_{2M} = \min\left(\varphi_2, \frac{\pi}{2} + \gamma - \eta_B\right),\ \eta_B = \eta(-\eta_B) \tag{44}$$

$$\eta_H \approx \eta_{H2} = \eta(\eta_{H1})\,,\ \eta_{H1} = \eta(0)\,,\ |\,\eta_H - \eta_{H2}\,| < 3.7\times 10^{-18} \tag{45}$$

$$\eta_B \approx \eta_{B2} = \eta(-\eta_{B1})\,,\ \eta_{B1} = \eta(0)\,,\ |\,\eta_B - \eta_{B2}\,| < 3.7\times 10^{-18} \tag{46}$$

$$\varphi_{1M} < \varphi_{2M} \Rightarrow set = \left[\frac{\varphi_{2M} - \varphi_{1M}}{\pi/180}\right] + 1,\quad \varphi_{MK} = \varphi_{1M} + \frac{\varphi_{2M} - \varphi_{1M}}{set} K \tag{47}$$

$$\varphi_{1M} \ge \varphi_{2M} \Rightarrow \int_{\varphi_1}^{\varphi_2} F_1(\varphi)d\varphi = 0\,,\ \varphi_{1M} < \varphi_{2M} \Rightarrow \int_{\varphi_1}^{\varphi_2} F_1(\varphi)d\varphi = \sum_{K=0}^{set-1}\left(\int_{\varphi_{MK}}^{\varphi_{M(K+1)}} F_1(\varphi)d\varphi\right) \tag{48}$$

Each summand within the integral sum by φ is calculated by substitution of subintegral function with a polynom of the 3[rd] degree[5] (polynomial method of the 3[rd] degree):

$$\int_{\varphi_{MK}}^{\varphi_{M(K+1)}} F_1(\varphi)d\varphi \approx \left(\frac{\varphi_{2M} - \varphi_{1M}}{set}\right)\frac{1}{8}\left(F_1(\varphi_{MK}) + 3F_1\left(\frac{\varphi_{MK}}{3/2} + \frac{\varphi_{M(K+1)}}{3}\right) + 3F_1\left(\frac{\varphi_{MK}}{3} + \frac{\varphi_{M(K+1)}}{3/2}\right) + F_1(\varphi_{M(K+1)})\right) \tag{49}$$

---

(5) In case of polynom of the 1[st] degree we would get a widely known method of trapezium. We were to refuse it, since its characteristical curve “truncation” of subintegral function would result in systematic error. The 3[rd] degree of polynom is minimal among degrees, which provide acceptable accuracy.

Integral $\int_{t_{nm1}}^{t_{nm2}} F_2(t)dt$ is taken by an interval at which the ecliptic longitude of the Sun center increments by 1 degree. This increment is close to a change of latitude at the pitch of integration by latitude. That is why it is natural to evaluate integral $\int_{t_{nm1}}^{t_{nm2}} F_2(t)dt$ in the same way, as integral $\int_{\varphi_{MK}}^{\varphi_{M(K+1)}} F_1(\varphi)d\varphi$, by method of the 3[rd] degree polynom:

$$\int_{t_{nm1}}^{t_{nm2}} F_2(t)dt \approx \frac{d_{nm}}{8}\left(F_2(t_{nm1}) + 3F_2(t_{nm4/3}) + 3F_2(t_{nm5/3}) + F_2(t_{nm2})\right) \tag{50}$$

As a result, practical evaluation of FVR integrals is performed based on secondary initial data by formulae (1), (40), (50), (41), (48), (49) with the use of (42)–(47), (35)–(39), (12)–(13), (7)–(10), (3)–(4).

3.6. Resulting roughnesses of evaluations

Resulting roughness of evaluation for each FVR integral will be at most few percents from average module of its interannual variability. Relative roughness does not exceed 0.005% for FVR integrals in the vicinity of poles and 0.00005% for FVR integrals in the vicinity of equator.

Subsequent to the results of evaluation for the period from 3000 BC till 2999 AD we formed a base of radiation data for arriving (in the absence of atmosphere) solar radiation to latitude zones of the Earth (5 degrees spread) with time pitch equal to 1/12 part of tropic year. Base of radiation data is set at the site “Solar radiation and climate of the Earth” (http://solar-climate.com/en/ensc/bazard.htm).

4. Secular trends in variation of arriving solar radiation

Secular variability has been evaluated by difference of arriving radiation values (J/m^2) during the last (2999 AD) and the first (3000 BC) year of the time interval for corresponding latitudinal zones. The results show the decrease for this period of solar radiation arriving to the outer fringe equal to 1.16E+09 J/m^2 or 0.339% from average annual value of solar radiation arriving during this period (Fedorov, 2012, 2015). This trend (fig. 1) is determined by secular variations of ellipticity, Earth axis inclination and longitude of perihelion (Milankovich, 1939).

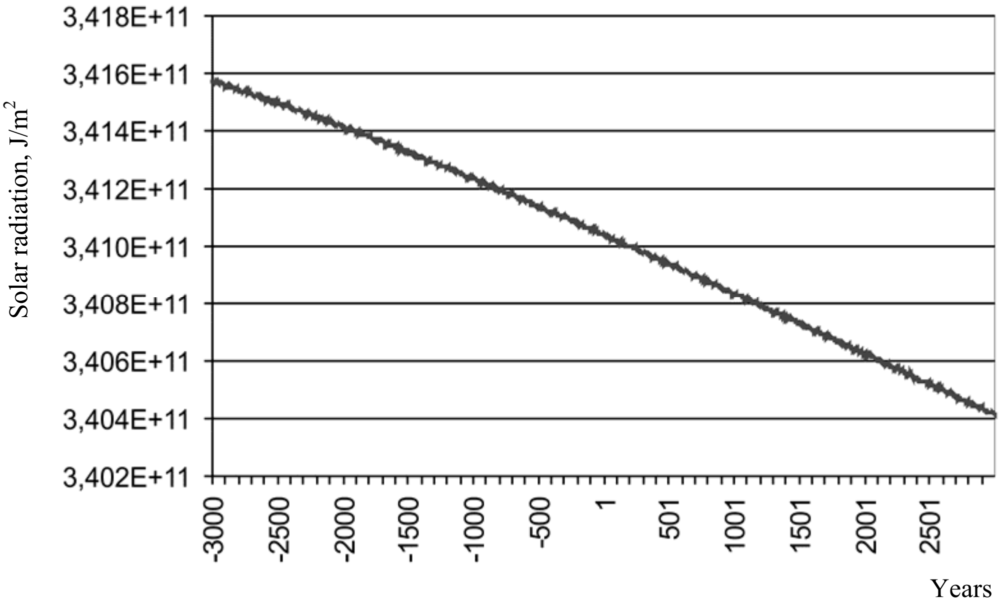

Fig. 1. Secular variation of solar radiation arriving to the Earth (in the absence of atmosphere) within the interval from 3000 BC till 2999 AD, J/m^2.

Reducing stream of solar radiation, arriving to the Earth ellipsoid during tropic year in districts below 45° of latitude at each hemisphere tends to increase and above 45° – to reduce (fig. 2).

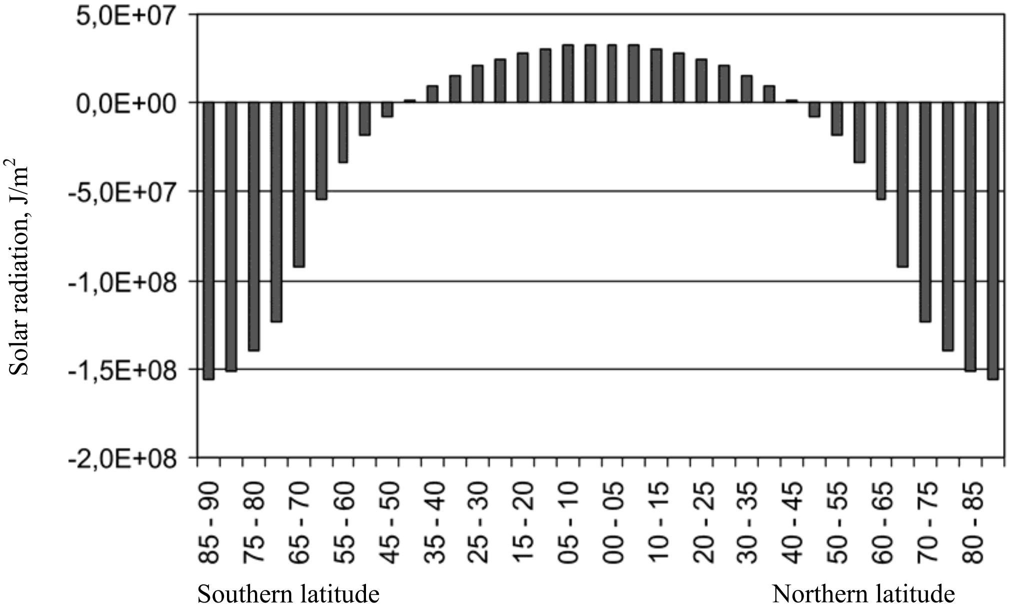

Fig. 2. Distribution of difference in solar radiation arriving to the Earth in the absence of atmosphere in 2999 and in 3000 BC to the corresponding latitudinal zones, J/m^2.

Reduction of radiation arriving to polar areas during the whole period achieves 1.58E+08 J/m^2, which is 2.8% in relation to average (for the whole interval) value of arriving radiation for latitudinal zones of 85°-90° geographic latitude. Increase within the equatorial area (exceeding polar districts by area, approximately by 2.7 times) is substantially smaller, and at equator region it equals to 3.32E+07 J/m^2 (0.25%). Consequently, one of the trends in variation of arriving solar radiation at present day is intensification of latitudinal contrast (increase of inter latitude gradient of solar radiation arriving to the outer fringe).

We also analysed solar radiation arriving to the outer fringe during winter and summer semester. Secular variation was evaluated by difference of values of arriving solar radiation (J/m^2) during the last (2999 AD) and the first (3000 BC) year of the time interval for corresponding semesters. During winter semester (for Northern hemisphere) (fig. 3) we registered decrease of arriving solar radiation within the latitudinal area from 10° S.l. to 90° S.l.

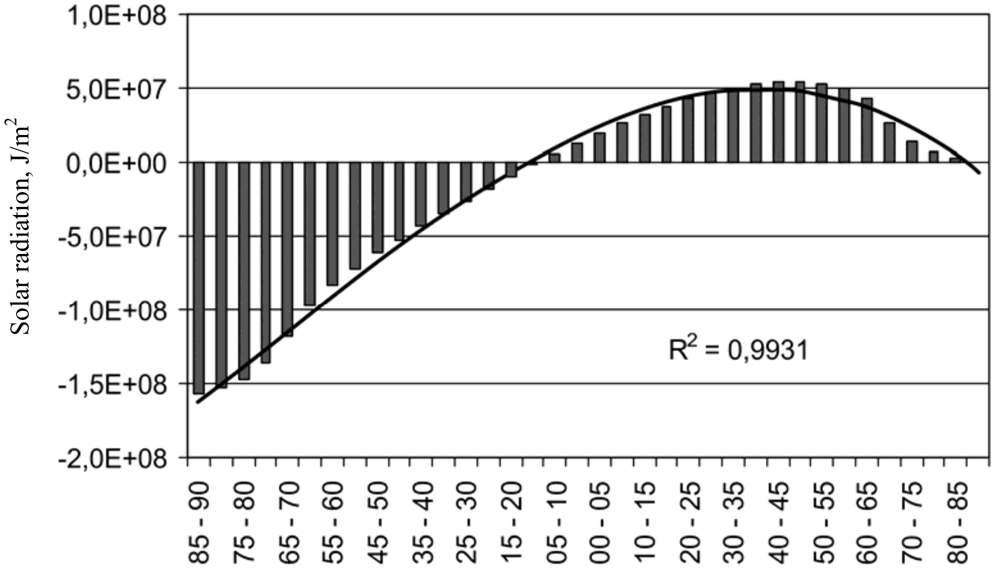

Fig. 3. Distribution of difference in solar radiation arriving to the Earth in the absence of atmosphere in 2999 and in 3000 BC in winter semester (for the Northern hemisphere) to the corresponding latitudinal zones, J/m^2. Approximation is 3rd degree polynom.

The decrease achieves the maximum value in this season in the Southern polar area -1.56E+08 J/m^2, which equals to 2.83% from the average annual (for the whole period) value of solar radiation arriving to this latitudinal zone. Decrease average for the 5-degree latitudinal zone during this interval (3000 BC-2999) equals to -7.55E+07 J/m^2. Total decrease of arriving radiation in the area of decrease is 1.21E+09 J/m^2. Positive values during this season are characteristic for the area of 5°-10° of the Southern latitude and for all latitudinal zones to the north from this zone. Maximum value is marked in latitudinal zone of 45°-50° N.l. is 5.42E+07 J/m^2, which equals to 2.04% of average annual value of radiation arriving to this zone in winter semester (for the Norhtern hemisphere). Increase, average for 5-degree zone, of arriving solar radiation equals to 3.14E+07 J/m^2. Increase within the area of increase is characterised by value equal to 6.29E+08 J/m^2. Overall decrease of solar radiation arriving to the Earth (to the outer fringe) during winter semester (for the Northern hemisphere) equals to -5.79 J/m^2.

During summer semester (for the Northern hemisphere) (fig.4) increase of arriving solar radiation is marked in the area from the zone of 5°-10° N.l. and situated to the south.

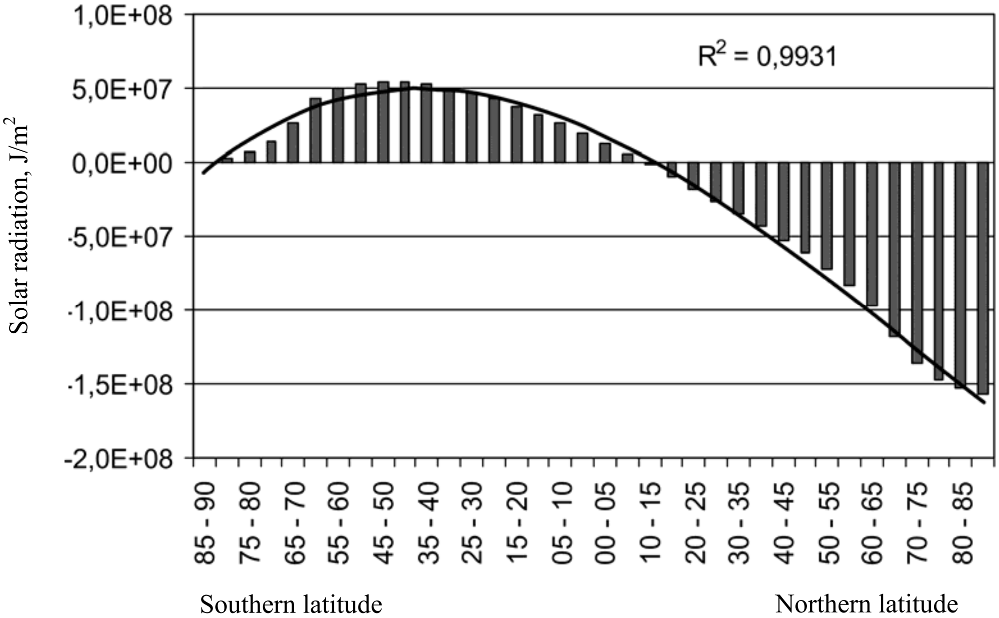

Fig. 4. Distribution of difference in solar radiation arriving to the Earth in the absence of atmosphere in 2999 and in 3000 BC in summer semester (for the Northern hemisphere) to the corresponding latitudinal zones, J/m^2. Approximation is 3rd degree polynom.

Maximum increase is a characteristic of the latitudinal zone of 45°-50° S.l. is 5.41E+07 J/m^2, which equals to 2.038% of average annual value of solar radiation arriving to this zone in summer semester (for the Norhtern hemisphere). Medium increase, for 5-degree latitudinal zone, in this area equals to 3.14E+07 J/m^2, and total (for the area of increase) equals to 6.29E+08 J/m^2. Decrease is marked at this time in the area of 10°-15° N.l. and to the north. Maximum decrease is a characteristic of the zone of 85°-90° N.l. and equals to -1.56E+08 J/m^2, which is 2.831% from average annual value of solar radiation arriving to this zone. Decrease, average for the 5-degree zone, equals to -7.55E+07 J/m^2, total (for the decrease area) is -1.21E+09 J/m^2. Total decrease (for the Earth) of arriving solar radiation in summer semester (for the Northern hemisphere) equals to -5.79E+08 J/m^2.

Thus, increase of arriving solar radiation is marked in winter semesters (for hemispheres), and decrease is marked in summer hemispheres. Seasonal variations of solar radiation arriving to the outer fringe are hereby flattened.

The marked trends (intensification of latitudinal contrast and flattening of seasonal differences) in variation of arriving solar radiation are connected with secular tendency towards decrease of the Earth axis inclination (regarding perpendicular to ecliptic plane) as a result of precession and nutation. It is known, that in case of the Earth's axis inclination increase, radiation arrival to polar regions increases, i.e. latitudinal contrast flattening and seasonal differences intensification takes place in hemispheres. In case of gradient angle decrease radiation will grow in subequatorial regions, resulting in intensification of latitudinal contrasts, and flattening of seasonal differences (Milankovich, 1939; Monin, Shishkov, 2000)

Conclusion

Based on astronomical ephemerides DE-406 evaluations of solar radiation arriving to the Earth ellipsoid have been performed (in the absence of atmosphere). Analysis of calculated values of arriving solar radiation allowed to obtain a number of interesting results:

1. Solar radiation arriving during tropic years to the outer fringe decreases.
2. Marked increase of solar radiation arriving to the Earth equatorial areas and decrease in polar areas. It means that the contemporary epoch is characterised with intensification of interlatitudinal gradient in distribution of arriving solar radiation at the outer fringe.
3. Marked decrease of arriving solar radiation in summer semesters and increase in winter ones (for hemispheres). This reflects a tendency of seasonal differences flattening in solar radiation arriving to the outer fringe.
4. Formed database of solar radiation arriving to the outer fringe (http://solar-climate.com/en/ensc/bazard.htm). These data may be used in physical and mathematical models of climate.

The obtained picture of temporal and spatial changes in solar radiation arriving to the Earth may find reflection in radiation and thermal conditions of the planet. In such a way, tendency to the increase of interlatitudinal gradient of arriving solar radiation may be connected with increase of interlatitudinal temperature contrasts and intensification of interlatitudinal heat exchange, which is possibly one of the reasons for the trend of climate warming in extra tropical regions of the Earth.

References

1. Макарова Е.А., Харитонов А.В., Казачевская Т.В. Поток солнечного излучения. – М.: Наука, 1991. – 400 с.

2. Миланкович М. Математическая климатология и астрономическая теория колебаний климата. – М.–Л.: ГОНТИ, 1939. – 208 с.

3. Монин А.С., Шишков Ю.А. Климат как проблема физики // Успехи физ. наук. 2000. – Т. 170. – № 4. – С. 419 – 445.

4. Шараф Ш.Г., Будникова Н.А. Вековые изменения орбиты Земли и астрономическая теория колебаний климата // Труды Института теоретической астрономии АН СССР, 1969. – вып. 14. – с. 48 – 84.

5. Berger A., Loutre M.F. Insolation values for the climate of the last 10 million years? // Quatern. Sci. Rev., 1991. – V. 10. – P. 297 – 317.

6. Berger A., Loutre M.F. Insolation values for the climate of the last 10 million years? // Quatern. Sci. Rev., 1991. – v. 10. – pp. 297 – 317.

7. Borisenkov E. P., Tsvetkov A.V., Agaponov S.V. On some characteristics of insolation changes in the past and the future // Climatic Change, 1983. – № 5. – P. 237 – 244.

8. Brouwer D., Van Woerkom A.J.J. The secular variation of the orbital elements of the principal planets // Astronomical Papers, 1950. – v. 13. – pp. 81 – 107.

9. Fedorov V.M. Interannual Variability of the Solar Constant // Solar System Research, 2012. – V. 46. – № 2. – P. 170 – 176. DOI: 10.1134/S0038094612020049.

10. Fedorov V.M. Periodic Perturbations and Small Variations of the Solar Climate of the Earth // Doclady Earth Sciences, 2014. – Vol. 457. – Part 1. – pp. 868 – 871. DOI: 10.1134/S1028334X14070137

11. Fedorov V.M. Latitudinal variability of incoming solar radiation in various time cycles // Doclady Earth Sciences, 2015. – Vol. 460. – Part 1. – pp. 96 – 99. DOI: 10.1134/S1028334X15010183

12. Foukal P., Fröhlich C., Spruit H., Wigley T. M. L. Variations in solar luminosity and their effect on the Earth's climate // Nature, 2006. – v. 443. – pp. 161 – 166. DOI: 10.1038/nature05072.

13. Fröhlich C., Lean J. The Sun’s Total Irradiance, Cycles, Trends and Related Climate Change Uncertainties since 1976 // Geophysical Research Letters, 1998. – v. 25. – № 23. – pp. 4377 – 4380.

14. Frohlich C. Solar Irradiance Variability // Atmospheric Research., 1989. – v. 23. – pp. 379 – 390.

15. Giorgini J.D., Yeomans D.K., Chamberlin A.B., Chodas P.W., Jacobson R.A., Keesey M.S., Lieske J.H., Ostro S.J., Standish E.M., Wimberly R.N. "JPL's On-Line Solar System Data Service", Bulletin of the American Astronomical Society **28**(3), 1158, 1996.

16. http://ssd.jpl.nasa.gov. – NASA, Jet Propulsion Laboratory California Institute of Technology (JPL Solar System Dynamics). Электронный ресурс национального аэрокосмического агентства США.

17. http://www.sidc.be/

18. http://www.pmodwrc.ch/

19. http://www.solar-climate.com/en/ensc/bazard.htm

20. http://ssd.jpl.nasa.gov/?horizons_doc#specific_quantities

21. Vulis, 1., Monin A.S. A contribution to the astronomical theory of variations of the climate of the Earth / Izv. Acad. Sci. USSR, Atmos. Ocean. Phys., 1979. – № 15. – pp. 3 –11. (ln English translation, 15, 1 – 9).

22. Willson R.C. Solar irradiance variations and solar activity // J. Geoph. Res., 1982. – 86. – pp. 4319 - 4326.

23. Willson R. C., Mordvinov A.V. Secular total solar irradiance trend during solar cycles 21 and 22 // Geophys. Res. Let., 2003. – 30. – 1199–1202. DOI: 10.1029/2002GL016038